A&A 441, 443–450 (2005)
DOI: 10.1051/0004-6361:20052877
© ESO 2005

Astronomy & Astrophysics

Photometric monitoring of the doubly imaged quasar UM 673: possible evidence for chromatic microlensing*

Th. Nakos[1,2,3], F. Courbin[4], J. Poels[2], C. Libbrecht[2,3], P. Magain[2], J. Surdej[2,**], J. Manfroid[2], I. Burud[5], J. Hjorth[6], L. Germany[1], C. Lidman[1], G. Meylan[4], E. Pompei[1], J. Pritchard[7,6,1], and I. Saviane[1]

[1] European Southern Observatory, Casilla 19001, Santiago, Chile
[2] Institut d'Astrophysique et de Géophysique, Université de Liège, Allée du 6 Août 17, Sart Tilman, Bât. B5C, 4000 Liège, Belgium
e-mail: nakos@astro.ulg.ac.be
[3] Royal Observatory of Belgium, Ringlaan 3, 1180 Brussels, Belgium
[4] Laboratoire d'Astrophysique, École Polytechnique Fédérale de Lausanne (EPFL), Observatoire, 1290 Sauverny, Switzerland
e-mail: frederic.courbin@epfl.ch
[5] Space Telescope Science Institute, 3700 San Martin Drive, Baltimore, MD 21218, USA
[6] Niels Bohr Institute, University of Copenhagen, Juliane Maries Vej 30, 2100, København Ø, Denmark
[7] Mount John University Observatory and Department of Physics & Astronomy, University of Canterbury, Private Bag 4800, Christchurch, New Zealand

Received 14 February 2005 / Accepted 3 June 2005

Abstract. We present the results of two-band CCD photometric monitoring of the gravitationally lensed quasar Q 0142−100 (UM 673). The data, obtained at ESO-La Silla with the 1.54 m Danish telescope in the *Gunn i*-band (October 1998−September 1999) and in the Johnson *V*-band (October 1998 to December 2001), were analyzed using three different photometric methods. The light-curves obtained with all methods show variations, with a peak-to-peak amplitude of 0.14 mag in *V*. Although it was not possible to measure the time delay between the two lensed QSO images, the brighter component displays possible evidence for microlensing: it becomes bluer as it gets brighter, as expected under the assumption of differential magnification of a quasar accretion disk.

Key words. gravitational lensing – quasars: individual: Q 0142−100 (UM 673)

1. Introduction

UM 673 (Surdej et al. 1987) is one of the first gravitational lens systems (GLs) found in a systematic optical search. It consists of two lensed quasar images ($z_s = 2.719$) separated by 2.2″. Although no direct spectrum of the lensing galaxy has ever been obtained, CaII and NaI absorption lines, detected in the spectrum of the fainter quasar image B, suggest that it is at a redshift $z_l = 0.49$ (Surdej et al. 1988; Smette et al. 1992). Because of its relatively bright apparent magnitude ($m_R(A) \sim 16.5$, $m_R(B) \sim 19.0$) and because of the wide angular separation between its images, UM 673 is a good target for a photometric monitoring program. The expected time-delay is of the order of a few months, which is relatively easy to measure, providing that the quasar itself displays significant photometric variations.

UM 673 has been monitored at the European Southern Observatory (ESO, La Silla, Chile) from 1987 to 1993 with several telescopes, leading to photometric measurements for 18 epochs. Unfortunately, the small field of view (FOV) accessible with CCDs in the eighties and the subsequent lack of PSF stars, restricted the effectiveness of the observations to unveil any weak variation, at the level of a few tenths of a magnitude (Daulie et al. 1993).

Within the framework of the Hamburg Quasar Monitoring Program (Borgeest & Schramm 1993), UM 673 has also been observed from 1988 to 1993 with the 1.23 m MPIA telescope, at Calar Alto Observatory, Spain. In contrast with Daulie et al. (1993), a *preliminary* analysis led to the detection of variations in the light-curve of component A, with a peak-to-peak amplitude of the order of 0.2 mag.

Sinachopoulos et al. (2001) reported variation of up to 0.5 mag over several years. Nevertheless, their data were irregularly distributed and the small size of the telescopes used, under moderate seeing conditions, only allowed the measurement of the *total* flux of the gravitational lens system.

* Based on observations made with the Danish 1.5 m telescope (ESO, La Silla, Chile) (Proposals: 63.O-0205(A), 64.O-0235(B), 65.O-0214(B), 66.A-0203(B), 67.A-0115(B), 68.A-0109(B)).
** Directeur de recherche honoraire du Fonds National de la Recherche Scientifique (Belgium).

Article published by EDP Sciences and available at http://www.edpsciences.org/aa or http://dx.doi.org/10.1051/0004-6361:20052877

The latest work on UM 673 (Wisotzki et al. 2004) reported on spectra obtained in September 2002. The data were taken with the 3.5 m telescope at Calar Alto (Spain), using the Potsdam Multi-Aperture Spectrophotometer (PMAS). By measuring the emission line to continuum flux ratios for the two quasar images, they concluded that, during the period of observations, no microlensing signature was detectable.

UM 673 was part of a photometric monitoring program carried out at ESO-La Silla, using the 1.54 m Danish telescope. In this monitoring, the photometric variability of several GL systems was first tested for a few months and the object was either followed up further in order to measure the time-delay (see for example Burud et al. 2002a), or stopped due to insufficient photometric variability. UM 673 is one of the objects that was stopped. However, it turned out to be interesting, after a more detailed analysis of the data was carried out. Both components show variability on long time-scales, with peak-to-peak variations of the order of 0.14 and 0.08 mag, in V and i respectively. While further (spectroscopic) observations will be needed to discriminate between intrinsic and microlensing induced variability, it is argued, on the basis of color information, that at least part of the variability, on time-scales of a few months, is likely due to microlensing.

2. Observations

The observations of UM 673 were carried out on a weekly basis using the Danish 1.54 m telescope at La Silla (Chile); at least three CCD frames were taken each night for each filter. In total, 63 CCD frames were obtained in the *Gunn i* filter, corresponding to 18 observing nights, from October 3, 1998 to September 29, 1999. In the Johnson V-band, 91 CCD frames were obtained, corresponding to 23 nights. 18 out of these 23 V-band epochs were taken during the same nights as the 18 *Gunn i* CCD frames. The remaining 5 V-band epochs were obtained between August 29 to December 15, 2001.

The CCD mounted on DFOSC (Danish Faint Object Spectrograph Camera) until September 2000 was a backside illuminated LORAL/LESSER chip, with a pixel scale of $0\farcs39$ pixel^{-1} and a field of view of 13.7×13.7 arcmin^2. This detector was then replaced by an EEV/MAT chip, with the same pixel scale and FOV. The exposure time for the individual CCD frame (>3 per epoch) in *Gunn i* was 250 s. For the V-band data, the integration time was varying between 150 and 600 s depending on the moon light and seeing, with 50% of the frames having an exposure time of 250 s. No data were lost due to bad weather conditions, thanks to the flexible scheduling applied during this observing program. Figure 1 shows a part of a typical *Gunn i* CCD frame. UM 673 can be identified on the north-east part of the field. Two neighboring stars, labeled S1 and S2, extensively used during the data reduction, are also indicated.

3. Data reduction techniques

We performed the photometric reduction and analysis using three different numerical methods to treat with photometry of blended objects. All three methods were developed at the Institute of Astrophysics and Geophysics of the University of Liège. The first one, the so-called *MCS*, is based on deconvolution (Magain et al. 1998). It has been extensively used to obtain the light-curves of many lensed quasars (e.g. Burud et al. 2002a,b). The second method, *Differential Imaging*, is based on a matching kernel technique similar to that developed by Phillips & Davis (1995). The last method, *General*, is a profile fitting technique that has been used to analyse data of lensed quasars, e.g., by Remy (1996) and Courbin et al. (1995).

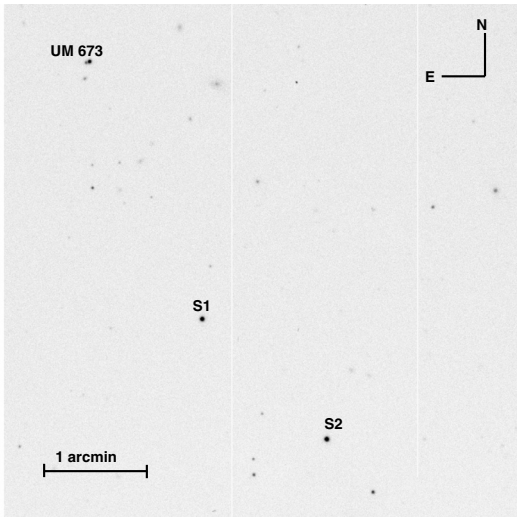

Fig. 1. Part of one *Gunn i* DFOSC CCD frame of UM 673. The field of view is $5' \times 5'$. Two reference stars are indicated (S1 and S2). Star S1, whose absolute photometry is well known (Nakos et al. 2003) has been used to normalize the CCD frames. Star S2 was taken as a comparison star.

Prior to the photometric analysis itself, all frames were preprocessed, i.e. bias-subtracted, flat-fielded and rescaled to the same pixel-coordinate reference system, using standard IRAF[1] procedures. Sky subtraction was performed using SExtractor (Bertin 1996), which can treat complicated sky structures, by removing the objects from the data and by estimating the sky background through a grid of cells adapted to the object density of the field. In the case of UM 673, the process resulted in a very accurate sky subtraction, at the percent level, due to the low stellar density and to the small spatial variations of the sky value in the original data.

The PSF varies significantly across the DFOSC field of view and the observed variation changes from one frame to another. Because of the very low number of stars suitable for the PSF determination, it was not possible to properly take this effect into account. This is probably the major cause of photometric uncertainties in our results.

3.1. Image deconvolution

The main difference between the MCS (Magain et al. 1998) method and most others is the simultaneous deconvolution capability of the algorithm: the deconvolved image is computed

[1] Image Reduction and Analysis Facility – is written and supported at the National Optical Astronomy Observatories (NOAO).

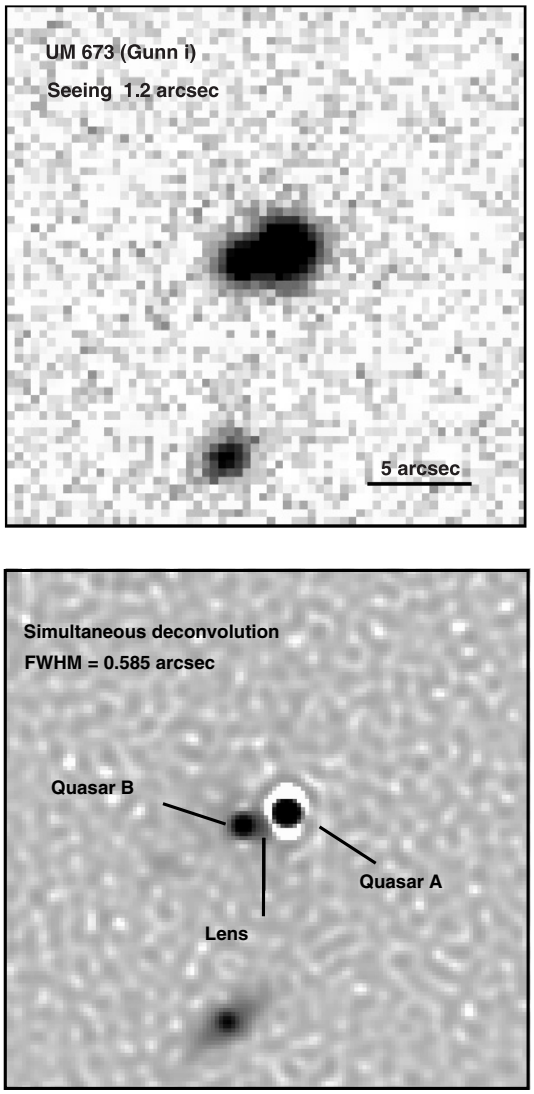

Fig. 2. *Upper panel*: a 25″ × 25″ region extracted from one of the 63 *Gunn i* CCD frames of UM 673. The seeing is 1.2″ and the pixel scale is 0.39″. *Lower panel*: simultaneous deconvolution of the 63 frames, with a final resolution of 0.585″ and a pixel size of 0.195″. Due to the PSF variations in the DFOSC field, minor artifacts were produced in the vicinity of the brighter quasar image. They represent only 0.5% of its peak intensity. The lensing galaxy is marginally seen between the two QSO components, close to component B. North is up, East is to the left. A logarithmic intensity scale has been used to display the images.

by minimizing the χ^2 between all the individual frames and a unique model image. The individual χ^2 corresponding to each image are minimized at the same time, hence the name of *simultaneous deconvolution*. All the available data are involved in this simultaneous fit, including those taken under mediocre observing conditions.

The deconvolved image is decomposed into a sum of analytical (Gaussian) point sources and a numerical deconvolved component which represents extended objects, such as the lensing galaxy or even the quasar host galaxy, if detected at all. In addition to the deconvolved image, the procedure returns the peak intensity and astrometric center of all point sources. The intensities are allowed to vary from one image to the next, hence leading to light-curves. The position of the point sources is forced to be the same in all images. The astrometry of the images with poor seeing is therefore constrained by the ones with better seeing.

The signal-to-noise of the final image is thus constrained by the whole dataset. It also has an improved spatial resolution, sampling and depth. Figure 2 compares a simultaneously deconvolved image with one of the original data, in the *Gunn i* filter. The chosen resolution is 0.585″ and the improved pixel size is 0.195″. The "ring" at the wings of the brighter component is due to strong PSF variations in the DFOSC field (see also Sect. 3.2). Its flux corresponds to ≈0.5% of component's A peak flux, for the *Gunn i*-band. For the *V*-band this effect is weaker, of the order of 0.1%.

Four stars in the vicinity of UM 673 were used to construct the PSF. A 64 × 64 pixel sub-frame, centered on UM 673, is extracted from each DFOSC frame. Prior to deconvolution, this sub-frame is flux-normalized, by division of the integrated flux of the non-variable star S1 (see Fig. 1). This cancels the effect of variable airmass and sky transparency. Star S2 is used as a comparison, in order to check the relative photometry, to control the errors and to quantify the effect of the PSF variations across the field. Both stars have been found to be photometrically stable (Sinachopoulos et al. 2001; Nakos et al. 2003). Unfortunately, no other bright, isolated star is present in the field of view.

The *Gunn i* and *V* fluxes of the two quasar components are converted to standard Johnson-Cousins magnitudes using the literature values of the reference star S2 (Nakos et al. 2003). We notice a slight shift between the *V* magnitude of S2 and the one published in the literature, probably due to differences in the apertures used to carry out the flux normalization relative to S1. The corrected value of the Cousins magnitude of S2 is 0.04 fainter than in Nakos et al. (2003), i.e. $V = 17.74 \pm 0.02$ and $(V - I) = 2.28$.

3.2. Differential imaging

The basic concept of this method, implemented in a new code (Python/IRAF/C++), contains elements taken from the IRAF task *psfmatch* (Phillips & Davis 1995). It is based on the comparison of a set of images, which have been registered and transformed so that their PSF and photometry perfectly match.

First, the best seeing and S/N image is identified and labeled as the reference image, all the other frames being called *input frames* in the following. All the frames are rescaled so that star S1 has a constant flux in all images.

The reference frame is subsequently degraded to match the resolution of the other frames. This is done by convolving the reference frame with a transformation kernel computed in the Fourier space. Each frame is then subtracted from the degraded reference, hence providing a residual frame showing only relative flux variations. Following this procedure, non-variable objects are removed, i.e. in the present case the contamination by the lensing galaxy is canceled.

Importantly, while this method provides accurate relative photometry, it does not give any information on the absolute photometric zero-point. This information is obtained by using the photometry from the PSF fitting method (see Sect. 3.3) as a cross calibration. Since the PSF fitting does not take the lensing galaxy into account, slight shifts are possible on the absolute scales adopted for the light-curves produced with MCS and with the differential imaging or PSF fitting method.

It is possible in the implementation of the code to use a convolution kernel that changes across the field of view. However, due to the very low number of useful PSF stars in the field of UM 673, a fixed kernel was used in the present application. Trial and error showed that the best kernel was obtained when star S1 alone was used for the computation. It is indeed the bright star closest to UM 673, for which the PSF variations are expected to be the smallest.

3.3. PSF fitting

"General" is a profile fitting technique that has already been applied to several gravitational lens systems (e.g., Burud et al. 1998; Østensen et al. 1997; Courbin et al. 1995). A set of field stars is used to construct a *numerical* profile to be fitted to the quasar components, together with a set of analytical profiles that represent extended objects. The advantage of this method is that it has few free parameters: the relative position and intensities of the quasar components, and the shape parameters of the lens (ellipticity, position angle). All parameters of the point sources and lensing galaxy are fitted simultaneously to the data.

The stars used to build the PSF for each frame are the ones labeled S1−S4 in Sinachopoulos et al. (2001) and Nakos et al. (2003). As for the other two methods, the flux of star S1 is taken as a reference to normalize all epochs.

The application of the method to the present data set was not straightforward, due to the large pixel size of the detector that hampers the accurate determination of the lens position. We therefore model UM 673 as two point sources only. The consequence is that the flux we measure for component B is contaminated by the lensing galaxy, even though the residuals after the simultaneous fit of the two PSFs to the quasar images are good. However, even with this contamination, the total summed fluxes of the two quasar images remain compatible with the flux measured through a large aperture applied directly to the data (see Fig. 6).

4. Results

The photometry of UM 673A and B, and of the reference star S2, is displayed in Figs. 3−5. Between 3 and 6 frames were obtained for each observing epoch and each filter. The values plotted in the figures are the mean values for each night. The 1σ error bar for each epoch is taken as the error on this mean value, i.e. the standard deviation between the magnitudes measured in the individual images at a given epoch, divided by $\sqrt{N}$, where N is the number of frames. The systematic errors due to the zero-point corrections, which are of the order of 0.02 mag, are not incorporated in the error bars.

On short time-scales, where both V and I-band data are available (see Figs. 3 and 4), all methods agree that component A shows a peak-to-peak variability of about 0.08 mag in the I-band, and about 0.14 mag in the Johnson V-band. The time scale of the variability is of the order of 350 days, for both filters. For component B, where the uncertainty in the photometry is larger, the short time-scale variability is at the limit of detection, for both filters. However, the five points around JD $\sim$ 1100, placed more than 3σ away from the points between JD $\sim$ 0 and JD $\sim$ 350, clearly show that, on larger time-scales, component B has also undergone photometric variations (see Fig. 5).

The comparison star S2 is used as an independent check of each photometric method. It is found that the dispersions between the photometric points (i.e. between all the epochs, as shown in Figs. 3−5) are compatible with the error bars estimated for each photometric method.

5. Discussion

5.1. Comparison of the methods

We have analyzed a two-band photometric data set of the gravitational lens system UM 673 (18 epochs in *Gunn i*, 23 epochs for the Johnson V-band), using three different photometric methods. All methods clearly reveal photometric variations, both over short (i.e. $\approx$350 days) and long (i.e. $\approx$1200 days) time scales. The variability of the brighter component A is well measured by all three methods, but is not as clear for the fainter image B.

The three photometric methods are applied to the data independently of any prior knowledge on the geometry of UM 673, e.g., as can be done from HST images (Lehár et al. 2000). This choice allows us to estimate the relative merits and drawbacks of the methods, especially with respect to the systematic errors, due to the PSF variations or to the design of the methods themselves. The only internal calibration applied is that the absolute flux ratio of the quasar images, as derived from the differential imaging, is determined by applying the absolute flux ratio from the PSF fitting method. The lensing galaxy is not taken into account in the PSF fitting. Our cross-calibration of one method using the other has no consequences on the V-band light-curves where the lens is faint. However, it has an effect on the I-band light-curves: Fig. 3 shows a systematic offset between the QSO light-curves obtained with MCS and the other two methods. The shift is in the opposite direction between images A and B. This effect is not present in the curves of the reference star S2 and is probably due to the contamination of the lens affecting the different methods in different ways. A zero-point miscalculation is excluded, since this would have resulted in the two curves moving in the same direction.

PSF variation or distortion does not have the same effect on the different methods. An outlier is seen, for example, in the I-band light-curve of star S2 when using the MCS method (I = 15.53), and corresponds to a set of images with bad focusing. This point is also an outlier in the PSF fitting light-curve and reveals a higher sensitivity of these methods to imperfect PSF determination.

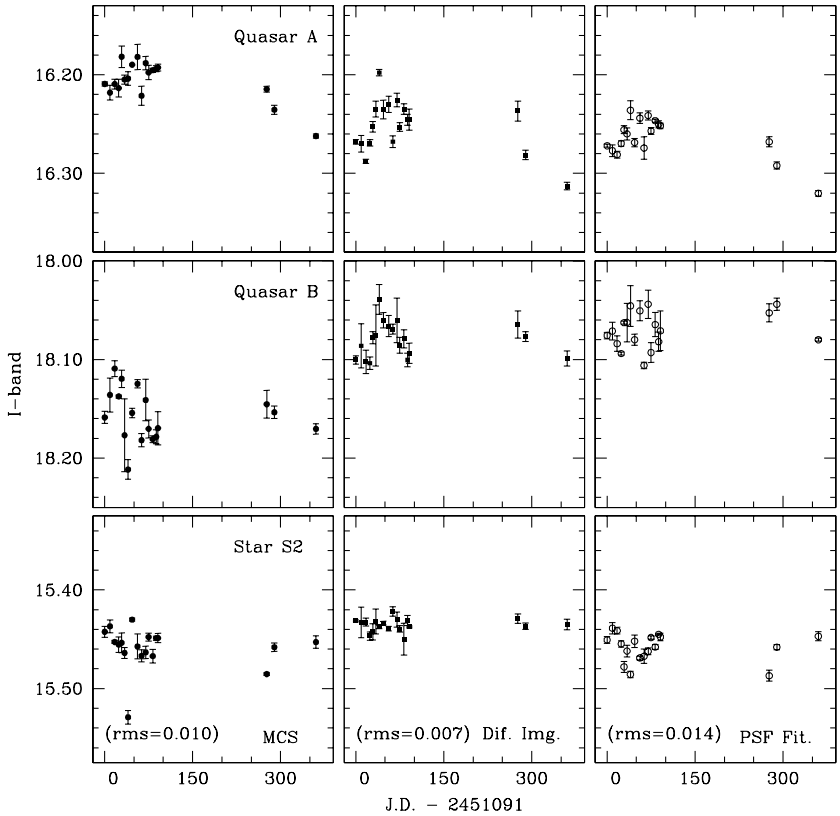

Fig. 3. Cousins *I*-band light-curves, for component A (*top*), component B (*middle*), and for the reference star S2 (*bottom*), as obtained from left to right with 1- the MCS deconvolution, 2- the Differential Imaging method, and 3- the PSF fitting method. The dispersion between the photometric points of star S2 is indicated in each panel. The Julian Date 2 451 091 corresponds to 1998, October 3.

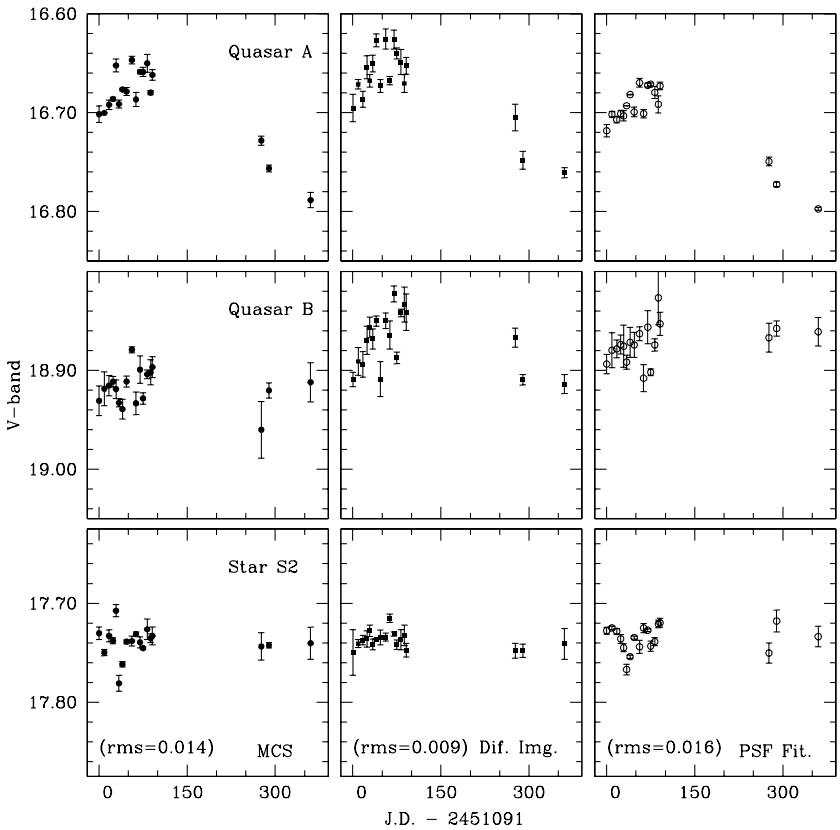

Fig. 4. Cousins *V*-band light-curves, spanning a period of 400 days (same symbols and organization as in Fig. 3). Each point corresponds to observations taken a few minutes before or after the *I*-band data shown in Fig. 3.

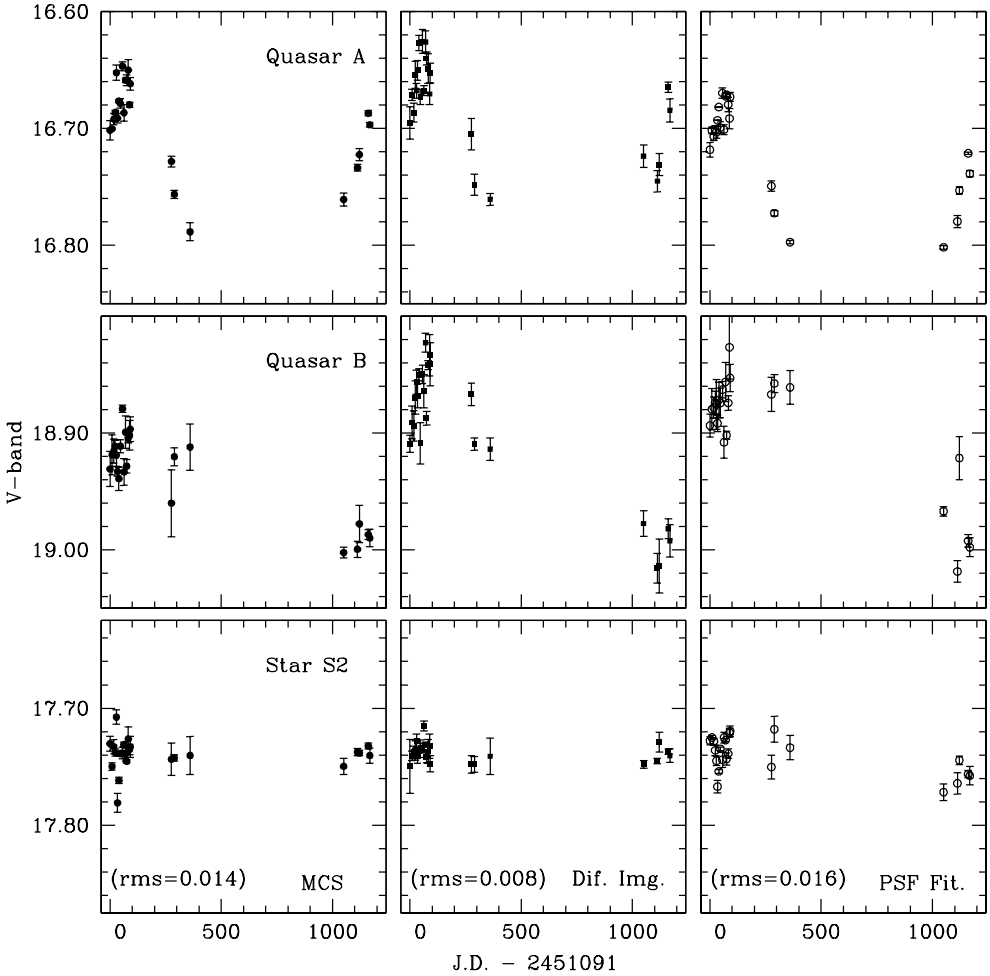

Fig. 5. Observations in the *V*-band were carried out for a longer time than the *Gunn i* ones, extending the light-curve up to 1200 days (same symbols and organization as in Fig. 3).

The systematic errors are consistent among the methods, but show a slight filter-dependence. In Fig. 6 we present the difference curve between the total light, as measured by direct aperture photometry of UM 673, and the sum of the fluxes of the two QSO components, as measured by the three methods. For the *I*-band (left panel), the points lie systematically above the mean value $\langle\Delta\mathrm{mag}\rangle = 0$, indicating that all methods overestimate the sum of the fluxes (A+B) at the level of 2%. For the *V*-band however (right panel), the spread of the points around the mean value $\langle\Delta\mathrm{mag}\rangle = 0$ is more homogeneous, leaving a hint that the presence of the galaxy in the *I*-band has an effect, although minor, in the photometric results obtained by the three methods.

5.2. The time delay

The parts of the light-curves that are the best sampled correspond to the 15 first measurements, spanning 120 days. Considering only this part of the curves and neglecting possible microlensing events, we have attempted to estimate the time delay between the quasar images. Unfortunately the peak-to-peak amplitude of the photometric variation is only 0.08 mag in the *V*-band and 0.05 mag in *I*, making it impossible to estimate the time delay. This is also the reason why it was decided to stop the observations of UM 673 after 3 months of monitoring, giving priority to other, more variable objects.

UM 673 shows larger photometric variations over longer time-scales, but these variations do not match at all after shifting the curve of component B relative to that of component A. These long term variations are sampled, in the *V*-band light-curves, with only three points at JD $\approx$ 350 days and with five points at JD $\approx$ 1100 days. The two groups of points span 150 days each. The fact that the light-curves do not match on long time scales has two possible interpretations: **1-** the time delay is longer than the length of the groups of points at JD $\approx$ 350 days and JD $\approx$ 1100 days, i.e. $\Delta t > 150$ days or, **2-** the variations are largely dominated by microlensing. We will see in the following that there is possible evidence supporting the latter interpretation rather than the former one, also given that predicted time delays for UM 673 are of the order of a few months (Surdej et al. 1988).

5.3. Evidence for microlensing

Although the large gaps in the light-curves of UM 673 do not allow the measurement of the time delay, the photometric

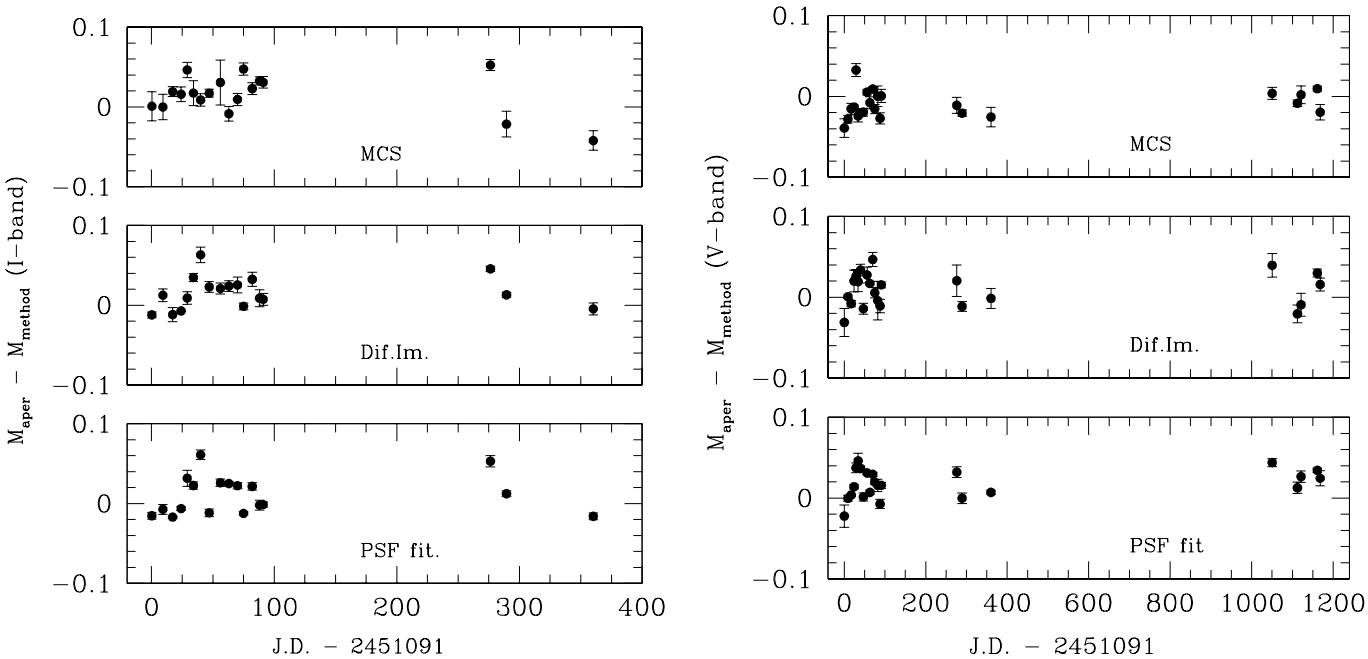

Fig. 6. *Left panel*: difference I-band light-curve between the aperture photometry and the magnitude corresponding to the sum of the fluxes of the two QSO components (A+B). The upper panel corresponds to the MCS algorithm, the middle panel is for the Differential Imaging, and the lower panel is for the PSF Fitting method. *Right panel*: idem for the V-band.

variations observed over long time scales are indicative of chromatic microlensing.

We have plotted in Fig. 7 the $V - I$ color index as a function of the V magnitude, for the two quasar images and for star S2, as derived with the three photometric methods. Since the error bars on the V-band photometry are comparable with the error bars on the I-band points, the distributions of points in Fig. 7 should be elliptical, with a long-axis parallel to the y-axis and $\sqrt{2}$ times larger than the (horizontal) short axis, in the case of no correlation between color and magnitude. While this is the observed situation for star S2, the plot for component A of the quasar displays a clear linear trend, indicating that it is becoming bluer as it gets brighter, in agreement with microlensing scenarios where a compact quasar accretion disk is (micro)lensed by a network of caustics. Microlensing preferentially amplifies the most central and bluer parts of the source with respect to more external and redder parts; an effect that can be seen in the continuum of a quasar spectrum (e.g. Wisotzki et al. 1993; Courbin et al. 2000).

This result is in apparent contradiction to the results of Wisotzki et al. (2004), who exclude the microlensing scenario from integral field spectroscopy, but their observations were performed in 2002. This is three years after the latest of the epochs of our light-curves where both V and I-band observations are available.

The reliability of the trend we observe in Fig. 7 can be tested by comparing the $V-I$ index obtained using one method, to the index measured by using the other two methods. If all methods are sensitive in the same way to a real $V - I$ trend as a function of the V magnitude, then the $V - I$ colors measured by two different methods should correlate well. If there is no real trend, the $V - I$ measurements are dominated by photon noise, and no correlation should be found. Doing this test reveals a strong correlation between the results in the three methods for quasar A, but not for quasar B or for the reference star S2. The color-dependent variations seen in the quasar image A can therefore be safely considered as real.

Although the case of microlensing being present for both components would be rather unusual, the color dependence on the V-band magnitude for component B, shown by differential imaging (Fig. 7), is quite puzzling and requires confirmation. Given the fact that none of the two other methods confirms the above trend, either higher signal-to-noise multicolor images are required, or an extensive high SNR spectrophotometric monitoring of UM 673.

If the variation we have observed is not due to microlensing, the peak-to-peak variation detected over three years is only 0.14 mag in the V-band. The photometric error on the individual points is about 0.01 mag for all three methods used in this paper and the visibility of UM 673 is about 6 months across the year. According to the simulations by Eigenbrod et al. (2005), the minimum sampling to adopt in order to derive the time-delay with an accuracy better than 2% in less than 2 years is of one point every three days, making UM 673 a very "expensive" object in terms of telescope time, if the goal is to use it to determine H_0. Given the chromatic variations detected in the present photometric monitoring, UM 673 may however turn out to be a very interesting object for microlensing studies.

Acknowledgements. We thank IJAF and ESO for granting us observing time for this project on a flexible basis. Th.N. acknowledges support from the project "Chercheurs Supplémentaires aux

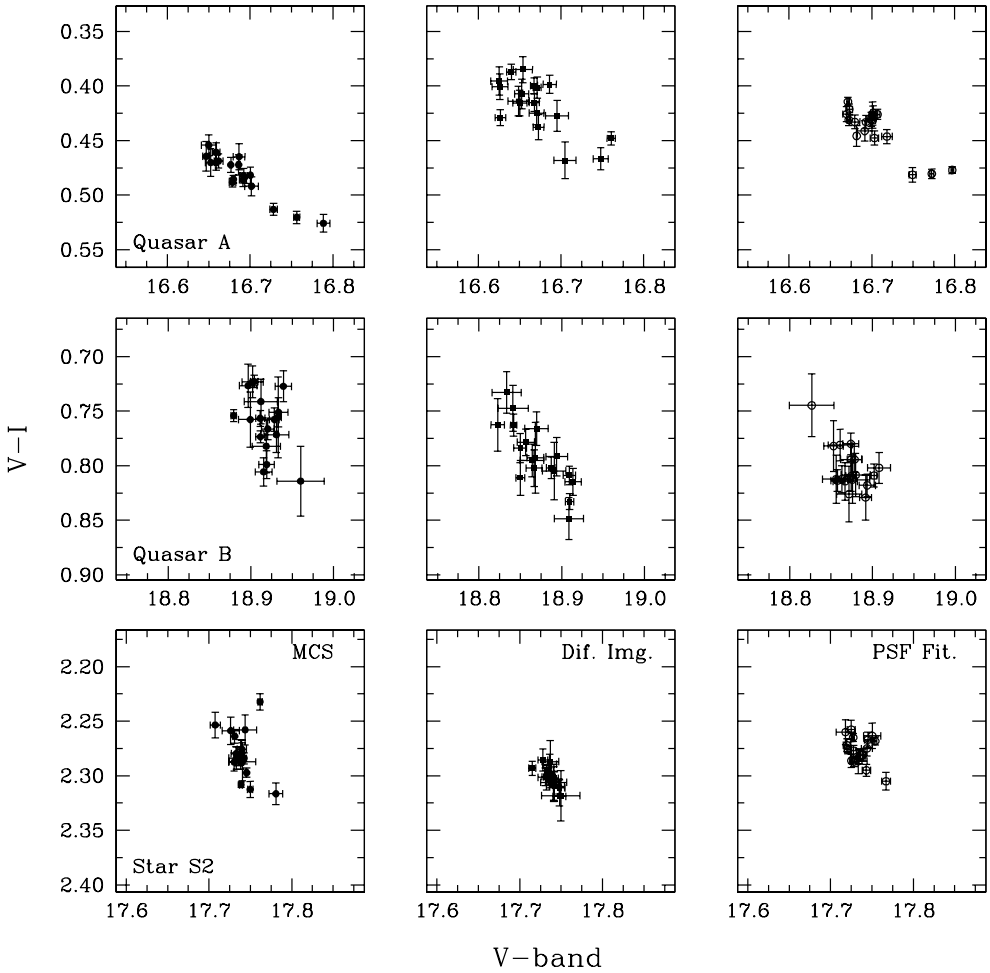

Fig. 7. Color ($V - I$) dependence of the photometric variations, for components A, B and for the reference star S2, as a function of the Johnson V magnitudes. A clear trend is visible for the quasar image A, becoming bluer when it is getting brighter.

Établissements Scientifiques Fédéraux". Part of the research was also performed in the framework of the IUAP P5/36 project, supported by the DWTC/SSTC Belgian Federal services. Th.N. also acknowledges C. Abajas Bustillo for the interesting discussions. F.C. acknowledges financial support Pôle d'Attraction Interuniversitaire, P4/05 (OSTC, Belgium). J.S. wishes to acknowledge support from the Belgian OSTC PRODEX program "Gravitational Lensing".

References

Bertin, E. 1996, A&AS, 117, 393
Borgeest, U., & Schramm, K. J. 1993, in Proc. 1st Megaphot Workshop, ed. U. Borgeest, K. J. Schramm, & J. von Linde, 105
Burud, I., Stabell, R., Magain, P., et al. 1998, A&A, 339, 701
Burud, I., Courbin, F., Magain, P., et al. 2002a, A&A, 383, 71
Burud, I., Hjorth, J., Courbin, F., et al. 2002b, A&A, 391, 481
Courbin, F., Magain, P., Remy, M., et al. 1995, A&A, 303, 1
Courbin, F., Lidman, C., Meylan, G., et al. 2000, A&A, 360, 853
Daulie, G., Hainaut, O., Hutsemékers, D., et al. 1993, Gravitational lenses in the universe, in 31st Liège International Astrophysical Colloquium, ed. J. Surdej et al., 181
Eigenbrod, A., Courbin, F., Vuissoz, C., et al. 2005, A&A, 436, 25
Lehár, J., Falco, E. E., Kochanek, C. S., et al. 2000, ApJ, 536, 584
Magain, P., Courbin, F., & Sohy, S. 1998, ApJ, 494, 452
Nakos, Th., Ofek, E. O., Boumis, P., et al. 2003, A&A, 402, 1157
Østensen, R., Remy, M., Lindblad, P. O., et al. 1997, A&AS, 126, 393
Phillips, A. C., & Davis, L. E. 1995, Astronomical Data Analysis Software and Systems IV, ed. R. A. Shaw, H. E. Payne, & J. J. E. Hayes, ASP Conf. Ser., 77, 297
Remy, M. 1996, Ph.D. Thesis, Liège University
Sinachopoulos, D., Nakos, Th., Boumis, P., et al. 2001, AJ, 122, 1692
Smette, A., Surdej, J., Shaver, P. A., et al. 1992, ApJ, 389, 39
Surdej, J., Swings, J.-P., Magain, P., et al. 1987, Nature, 329, 695
Surdej, J., Magain, P., Swings, J.-P., et al. 1988, A&A, 198, 49
Wisotzki, L., Köhler, T., Kayser, R., et al. 1993, A&A, 278, L15
Wisotzki, L., Becker, T., Christensen, L., et al. 2004, Astron. Nachr., 325, 135